Development of an optical approach for noninvasive imaging of Alzheimer's disease pathology

Jesse Skoch
Massachusetts General Hospital
MassGeneral Institute for Neurodegenerative Disease
Department of Neurology/Alzheimer's Disease Research Unit
114 16th Street
Charlestown, Massachusetts 02129

Andrew Dunn
Massachusetts General Hospital
Department of Radiology
Martinos Center for Biomedical Imaging
114 16th Street
Charlestown, Massachusetts 02129

Bradley T. Hyman
Brian J. Bacskai
Massachusetts General Hospital
MassGeneral Institute for Neurodegenerative Disease
Department of Neurology/Alzheimer's Disease Research Unit
114 16th Street
Charlestown, Massachusetts 02129
E-mail: bbacskai@partners.org

Abstract. Alzheimer's disease (AD) is characterized by the presence of aggregates of the amyloid-β (Aβ) peptide in the brain. These aggregates manifest themselves as senile plaques and cerebrovascular amyloid angiopathy (CAA). While traditional histochemical approaches can easily identify these deposits in postmortem tissue, only recently have specific ligands been developed to target Aβ in living patients using positron emission tomography (PET). Successful detection of Aβ pathology in patients will enable definitive preclinical diagnosis of AD, and enable quantitative evaluation of the efficacy of anti-Aβ therapeutics developed to treat the disease. PET scanning, however, has several disadvantages including high cost, low availability, and the requirement for radioactive tracers. We describe recent progress in the development of techniques for imaging Aβ deposits noninvasively using optical approaches. Successful development of an optical detection platform would enable inexpensive, accessible, nonradioactive detection of the Aβ deposits found in AD. © *2005 Society of Photo-Optical Instrumentation Engineers.* [DOI: 10.1117/1.1846075]

Keywords: amyloid-β; spectroscopy; microscopy; positron emission tomography ligand; Alzheimer's disease; near infrared; noninvasive imaging.

Paper NEU-02 received Feb. 20, 2004; revised manuscript received Apr. 28, 2004; accepted for publication May 6, 2004; published online Feb. 3, 2005.

1 Introduction

Definitive diagnosis of Alzheimer's disease (AD) in living patients has been a goal since the first description of the disease in 1906. While experienced neurologists can diagnose AD with an accuracy approaching 90%, an examination of the postmortem brain is still required for substantiation. Neuropathological examination of brain tissue relies on detection of senile plaques, neurofibrillary tangles, and neuronal loss for definitive diagnosis.[1–3] Senile plaques are large extracellular aggregates of the amyloid beta (Aβ) peptide, a 39–43 amino acid fragment derived from the amyloid precursor protein[4,5] (APP). Aβ accumulates with a β-sheet structure in mature plaques, enabling histochemical detection with a variety of compounds that bind to β-sheets, including thioflavin S, thioflavin T, and congo red.[6] Neurofibrillary tangles (NFTs) are intracellular structures comprised primarily of a different misfolded protein called tau.[7] Mature NFTs also have a tertiary structure that enables detection with the histochemical stains thioflavin S, thioflavin T, and congo red.[1–3] Despite the availability of these stains for the pathologies found in AD brain tissue, no existing compound has been suitable for diagnostic use in humans, primarily because of the requirement to cross the blood-brain barrier (BBB) to enter the central nervous system (CNS). This obstacle has only recently been overcome to allow radiotracer detection of plaque binding with positron emission tomography[8,9] (PET). The most promising tools are rationally designed derivatives of known amyloid binding compounds to enable entry into the CNS. Pittsburgh compound B (PIB) is a smaller, more lipophilic derivative of thioflavin T and is currently being evaluated for PET imaging in humans.[9,10] PIB retains the affinity and specificity for amyloid plaques of the parent compound, but enters and clears the brain very quickly.[11] Ligand that binds amyloid deposits does so with high affinity and is retained for up to several days. PIB is fluorescent, enabling characterization in mouse models using multiphoton microscopy.[10,11] In preparation for multiphoton imaging, mice were surgically prepared with a cranial window comprised of a glass cover slip cemented in place of the skull. This procedure is somewhat invasive, but enables both acute and chronic imaging of fluorescently labeled structures up to several hundred micrometers deep into the brain with spatial resolution of the order of 1 μm. High spatial resolution enables direct histochemical confirmation of labeled structures and therefore characterization of the specificity of the ligand binding in living animals. Unfortunately, the extremely high spatial resolution obtained with multiphoton microscopy along with limited depth penetration prohibit acquisition of whole-brain images. While imaging techniques such as PET, single-photon-emmission computed tomography (SPECT), and magnetic resonance imaging (MRI) are able to acquire whole brain images noninvasively, the spatial resolution of these techniques is several orders of magnitude less than that of multiphoton imaging.[12]

Address all correspondence to Brian J. Bacskai, MassGeneral Institute for Neurodegenerative Disease, Massachusetts General Hospital, Department of Neurology/Alzheimer's Disease Research Unit, Charlestown, MA 02129; Tel: 617-724-5306; Fax: 617-724-1480; E-mail: bbacskai@partners.org

1083-3668/2005/$22.00 © 2005 SPIE

Downloaded From: http://biomedicaloptics.spiedigitallibrary.org/ on 01/25/2016 Terms of Use: http://spiedigitallibrary.org/ss/TermsOfUse.aspx

While PET shows great promise for noninvasive amyloid imaging in humans, the technique has several disadvantages. First, it depends on radioactive ligands, although in only trace amounts. Second, the half-life of C^{11} compounds is about 20 min, requiring an on-site cyclotron for synthesis in specialized facilities. This limits the accessibility of the imaging technique. Third, the technique is expensive, prohibiting widespread screening of large patient populations. A successfully developed optical technique would overcome all of these limitations. Optical techniques do not require radioactive ligands, but would probably require higher concentrations of administered ligand. An optical detection platform could be portable, easily accessible anywhere, and commercially available near IR optical scanning units (currently used for blood flow measurements) are relatively inexpensive. Moreover, unlike microPET devices available only in specialized centers that have substantial infrastructure on site, optical imaging utilizing commercially available equipment is well suited for research applications with experimental models such as transgenic mice. Therefore, we have pursued alternatives to PET imaging that rely on optical detection. For deep tissue imaging, the near-IR (NIR) optical spectrum has distinct advantages due to the high transmission in biological tissues.[13] Operating in the range between the absorption peaks of hemoglobin (>650) and the absorption of water (<850) maximizes the depth penetration of NIR light, but significant scattering of both excitation and emission signals will occur. Sophisticated reconstruction techniques based on diffuse optical tomography can compensate and enable 3-D imaging of optical signals deep within biological tissue.[14,15] This paper describes progress toward developing optical detection strategies for noninvasive detection of senile plaques in intact animals as proof-in-principle that noninvasive optical imaging is feasible. Using model compounds for specific plaque targeting with NIR fluorescent properties, and existing commercial detection platforms, we show that optical detection can discriminate between plaque-containing and non-plaque-containing tissue and brains.

We evaluated four different existing commercial detection platforms to image NIR fluorescent probes in brain tissue from transgenic mice: a standard laser-scanning upright fluorescent microscope modified to use a NIR light source; a commercially available plate reader that utilizes NIR lasers; a ''gene array'' scanner that provides rapid, high-resolution images of a 1×3 microscope slide using several lasers, and a whole animal time-domain NIR imaging system. Each of the first three are commonly available laboratory equipment found in many research settings, that can be used for assay development and histological studies of amyloid plaques; the last is the laboratory equivalent of clinical instrumentation, enabling *in vivo* detection (with the appropriate contrast agent) of Aβ deposition and longitudinal studies.

2 Methods

2.1 *Immunohistochemistry*

Fixed (4% paraformaldehyde) tissue sections from aged[16] (>12 months) TG2576 mice were blocked in 3% milk in tris-buffered saline (TBS) for 1 h, incubated overnight with a 1:200 dilution of the monoclonal mouse antibody BAM-10 (Sigma, St. Louis) conjugated to Alexa Fluor 750 (Molecular Probes), and then washed in TBS. For whole brain immunohistochemistry fixed (4% paraformaldehyde) PDAPP (Ref. 17), Tg2576, and C57/BL6 brains were immersed in a 1:100 dilution of BAM-10 conjugated Alexa Fluor 750 in TBS containing 1.5% normal goat serum for 24 h. Brains were washed 3 times for 10 min in TBS.

2.2 *Animal Preparation*

All animals were prepared, maintained, and sacrificed humanely in accordance with the Subcommittee on Research Animal Care at Massachusetts General Hospital, and conform to the National Institutes of Health (NIH) guide for the care and use of laboratory animals. Mice were anesthetized with an intraperitoneal injection of Avertin (250 mg/kg), with supplemental doses (40 mg/kg) as needed. The head was shaved and aseptically treated with three alternating applications of Betadyne and 70% isopropyl alcohol. A subcutaneous injection of 2% Xylocaine local anesthetic preceded a 2-cm incision over the midline of the scalp (anterior to posterior). For cerebral injection, a 1-mm burr hole was drilled at 0.07 cm posterior to bregma and 0.15 cm right of the midline. Stereotaxic positioning was used for injections through a 28G Hamilton syringe. The syringe tip was lowered 0.3 cm, as measured from the skull surface. To prevent possible spillover, a low-melting-point wax was dripped over the needle/skull interface to form a seal. Then 8 μL of Alexa Fluor 750 conjugated BAM-10 antibody at 0.1 mg/mL in phosphate-buffered saline (PBS) was injected at 0.70 μL/min. To enable diffusion and prevent eruption of dye onto the skull surface, the syringe was left in place for 5 min after the injection before being slowly retracted. A PBS-saturated surgical Gelfoam cube (1 mm^3, Pharmacia/Upjohn—compressed) was immediately placed over the exposed burr hole to absorb any blood. After removing the Gelfoam, the scalp was sutured closed and the animal was imaged. The animal was allowed to recover on a thermally regulated heating pad.

2.3 *Laser Scanning Microscopy*

Stained tissue sections were mounted in aqueous mounting solution (GVA, Zymed) and imaged on an Olympus BX50 upright microscope with water immersion objectives. Fluorescent samples were excited with a tunable laser at 750 nm (MaiTai, Spectra Physics) scanned by a BioRad 1024 confocal system, and nondescanned fluorescence ($\lambda>780$ nm) was detected by an avalanche photodiode (APD, Hamamatsu).

2.4 *DNA Array Scanner*

Mouse brain sections were stained with 15 μM indocyanine green (ICG) (Sigma, St. Louis) in TBS for 10 min and then washed three times for 5 min in TBS. Afterward, the same sections were stained in 0.05% thioflavin S in TBS for 5 min followed by a dip wash in 80% ethanol and two 5-min washes in TBS. Sections were mounted in aqueous mounting solution on glass slides and imaged in a DNA microarray scanner (ScanArray Express, Perkin Elmer) with a 488-nm laser at 20 μm/pixel resolution.

2.5 *LI-COR Odyssey Imaging*

The LI-COR Odyssey plate scanner was adapted to take advantage of its large scanning area. Stained tissue sections

Downloaded From: http://biomedicaloptics.spiedigitallibrary.org/ on 01/25/2016 Terms of Use: http://spiedigitallibrary.org/ss/TermsOfUse.aspx

were mounted on slides and placed on the glass plate for imaging. *Ex vivo* brains were laid dorsal side down on the scanner surface and scanned with the device's 680- and 780-nm lasers simultaneously with an effective 21 μm/pixel resolution. Focus offsets from the scanner surface varied from 0 to 4 mm. For *in vivo* imaging, anesthetized animals were placed on their backs and restrained with a taught length of silk suture thread over the jaw, which resulted in the majority of the dorsal surface of the head being flush against the scan surface. Focus offsets from the scanner surface varied from 2 to 4 mm. For most *in vivo* scans, spatial resolution was sacrificed (42 μm/pixel) to decrease scan time.

2.6 *eXplore Optix Imaging*

The eXplore Optix imager is a commercial solution for molecular imaging in small animals and features time-domain imaging capabilities as well as excitation source/detector offset to account for deep tissue scattering of fluorescence. *Ex vivo* brain preps were secured to a petri dish with Krazy™ glue and immersed in TBS. Brains were scanned in groups of two simultaneously at 0.5-mm resolution with the scanning focal plane set just below the cortical surface. Changing the focal depth had only minor effects on the fluorescence intensity detected. For *in vivo* imaging, live animals remained anesthetized inside the imager during the 12- to 15-min period required to scan the head at 0.5-mm resolution. The scanning focal plane was typically set at mouse eye level.

3 Results

Recent successes in developing amyloid-targeting reagents for PET imaging of AD pathology in the brain are encouraging.[8–10,18,19] These amyloid-targeting reagents are derivatives of histological stains that are fluorescent in the range of ordinary laboratory fluorescent microscopes, usually in the blue region. NIR fluorophores offer advantages for deep detection of labeled structures through biological tissues because of the high transmission between[13] 650 and 850 nm. Therefore, our goal is to translate the blue fluorescent dyes into the NIR spectrum to achieve noninvasive optical imaging of senile plaques in living animals. To accomplish this goal, both NIR detection strategies as well as optimized plaque ligands must be developed.

We developed several lines of model near infrared contrast agents for use either with histological preparations or *in vivo*, based on their Aβ-binding characteristics, spectral properties, and ability to cross the BBB. We used a fluorescently labeled antiamyloid antibody as a model compound to evaluate detection platforms. Using Alexa Fluor 750 labeled antiamyloid beta (BAM-10) antibody, we created a model compound with ideal spectral properties, and ideal amyloid specificity. The labeled antibody is too large to cross the BBB in detectable amounts, however, preventing systemic administration in a living animal. We applied labeled antibody to thin sections from an aged mouse model of AD (18 month old Tg2576 mouse brain), and imaged the sections in two different ways. First, we utilized an Olympus BX50 upright microscope equipped with a tunable NIR laser ranging from 710 to 920 nm (MaiTai, Spectra Physics). We modified the emission collection assembly to enable single photon excitation at 750 nm, and emission collection with a 780-nm-long pass filter, focused onto the active area of an APD (Hamamatsu). The output from the APD was directed into the analog-to-digital (A/D) converter of a Biorad 1024ES microscope to enable seamless integration of the NIR signals with the existing scan hardware and software. This approach leads to somewhat out-of-focus fluorescence in thick specimens because it does not take advantage of confocal imaging, but it certainly is adequate to clearly detect objects the size of individual plaques (approximately 10 to 50 μm in diameter). Figure 1 shows an example from a tissue section of a transgenic mouse brain labeled with Alexa Fluor 750 conjugated BAM-10 antibody. The advantages of this approach result from the flexibility of the tunable laser, and the high spatial resolution inherent in the high-magnification, high-NA microscope objectives. This provides a versatile platform with which to examine potential NIR Aβ-binding compounds.

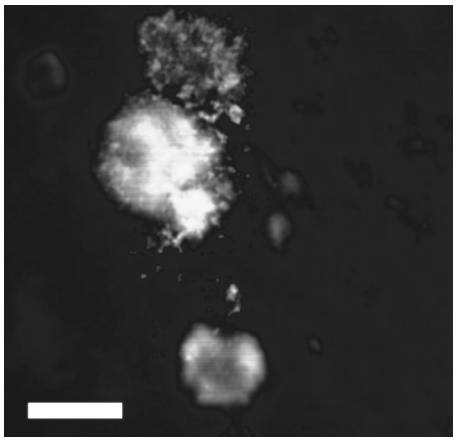

Fig. 1 NIR microscopy of immunohistochemically labeled plaques in mouse tissue. Tissue sections were cut from transgenic mouse brains and processed for immunohistochemistry. The tissue was treated with Alexa Fluor 750 conjugated BAM-10 antibody as a model compound for specific, NIR plaque targeting, and imaged using a modified laser scanning microscope and a tunable NIR excitation source. This image was acquired using a water immersion 20× objective [numerical aperture (NA)=0.5, Olympus]. The fluorescent objects are amyloid deposits within the section that are labeled with high contrast using the antibody. Scale bar=50 μm.

We adapted another instrument platform for fluorescence detection in histological sections: a DNA array reader (ScanArray™ Express, Perkin Elmer). The instrument scans slides with a maximal resolution of 5 μm/pixel with up to five lasers and matched emission filters. Figure 2(a) shows the resultant image from a scan using 488-nm excitation and 535-nm emission to detect plaques labeled with thioflavin S within a tissue section. Dense-core plaques are clearly and specifically labeled with this histochemical stain. The ability to obtain low-magnification scans of tissue using visible lasers will help to confirm the specificity of novel fluorescent probes with direct comparison to the established histochemical stain, thioflavin S. The ScanArray Express enables relatively high resolution scans of large areas with flexible fluorescent channel selection to enable screening and evaluation of the binding properties of fluorophores from the visible to the far-red spectrum. It will also be possible to modify the instrument by adding additional lasers and emission filters to enable tandem visible and NIR fluorescent scans.

Downloaded From: http://biomedicaloptics.spiedigitallibrary.org/ on 01/25/2016 Terms of Use: http://spiedigitallibrary.org/ss/TermsOfUse.aspx

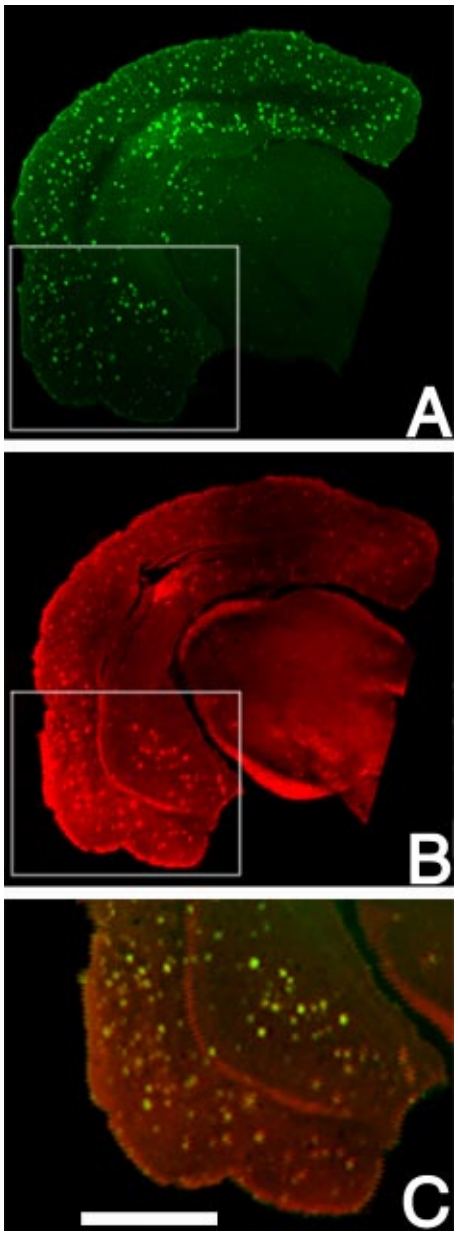

Fig. 2 Visible light scanning of the standard histochemical probe thioflavin S used to validate the specificity of amyloid binding with novel NIR probes. ICG labels a similar population of thioflavin S positive Aβ deposits. Tissue sections were cut from a transgenic mouse brain (PS1/APP) and processed for histochemistry. Sections were stained with the NIR fluorescent compound ICG followed by thioflavin S. (a) Thioflavin S was imaged using the Perkin Elmer ScanArray Express with a 488-nm laser line at a resolution of 20 μm/pixel. (b) The same section was imaged using an NIR plate reader (LI-COR Odyssey) at 780-nm excitation and 800-nm emission with a resolution of 21 μm/pixel to detect ICG localization. (c) Superimposition and enlargement of these two images indicate that ICG is colocalized with thioflavin S at the single plaque level albeit with somewhat less specificity. The scale bar is 1 mm.

We next evaluated another existing commercial device utilizing NIR lasers for fluorescence excitation. Figure 2(b) shows an image acquired using the LI-COR Odyssey™, a plate reader with two-channel fluorescence detection in the NIR. It is equipped with two continous wave diode lasers at 680 and 780 nm, and two APDs for NIR emission collection. The plate reader can scan an area of 21×21 cm, at a resolution up to 21 μm/pixel. Using tissue sections from the brain of a transgenic mouse that were stained with our NIR fluorescent model compounds, we were able to obtain images of labeled plaques within the sections. This detection scheme provides a rapid evaluation of the specificity of NIR fluorophores across a large area (a coronal section of one hemisphere of the brain, in this case) using two different wavelengths simultaneously at a resolution sufficient to detect microscopic structures.

We used this strategy to evaluate whether the commonly used NIR fluorophore ICG exhibited any specificity for plaque labeling in the brain. This chromophore has nearly ideal spectral properties, but is too large to cross the BBB. It should serve as a starting point for a small molecule with appropriate NIR spectrum for amyloid targeting in the brain. As shown in Fig. 2(b), ICG already shows some affinity for amyloid plaques in the brain. It binds to a subset of plaques, comparable to the population of dense-core plaques that are labeled with other histochemical stains like thioflavin S [Fig. 2(a)]. This result suggests that modifications to ICG to make it smaller and more lipophilic to enter the brain while maintaining the fluorescence spectrum may enable noninvasive amyloid imaging in the brain.

For noninvasive optical imaging in the brain, we sought to evaluate an instrument for detecting labeled structures within an intact brain, and not just a thin section cut from a brain. We incubated intact, fixed (postmortem) transgenic and age-matched nontransgenic brains in our model compound, Alexa Fluor 750-labeled BAM-10 antibody, overnight followed by extensive washing, to enable diffusion of the antibody several hundreds of micrometers deep into the brain. We placed these brains side-by-side in a dedicated small animal molecular imager (eXplore Optix™, Advanced Research Technologies, Inc.) and acquired fluorescence images. This device is designed for small, intact animal imaging using time-domain NIR fluorescence readouts. The system employed a picosecond-pulsed diode laser at 750 nm, with a photomultiplier tube (PMT) detector offset by 3 mm for diffuse optical tomography (DOT) reconstructions. The laser-scanning/PMT assembly scanned a region of interest (ROI) defined by coordinates overlaid onto a white-light image of the sample. Scattered fluorescence was collected through a 780-nm long-pass filter (Omega Optical). Extracted brain or mouse head scans took 8 to 12 min. As shown in Fig. 3, the intensity images of the two excised brains were different, with the transgenic brain having ~2× more signal. As would be expected with any *in vivo* optical images, the spatial resolution of the images is diminished considerably due to the high degree of scattering of both the excitation and emission light in the brain. Resolution and depth discrimination could be improved using image reconstruction, although only the raw intensity images are shown here. The background fluorescence is quite high in the transgene negative brain, most likely due to incomplete washing of the unbound fluorophore. Nonetheless, this image demonstrates that fluorescence from within an intact brain can be measured quantitatively with this near infrared laser scanning device. The image shown in Fig. 3 does not take advantage of the fluorescence lifetime capability of this instrument.

These images illustrate the potential for noninvasive, whole animal detection of specifically labeled plaques in the

Downloaded From: http://biomedicaloptics.spiedigitallibrary.org/ on 01/25/2016 Terms of Use: http://spiedigitallibrary.org/ss/TermsOfUse.aspx

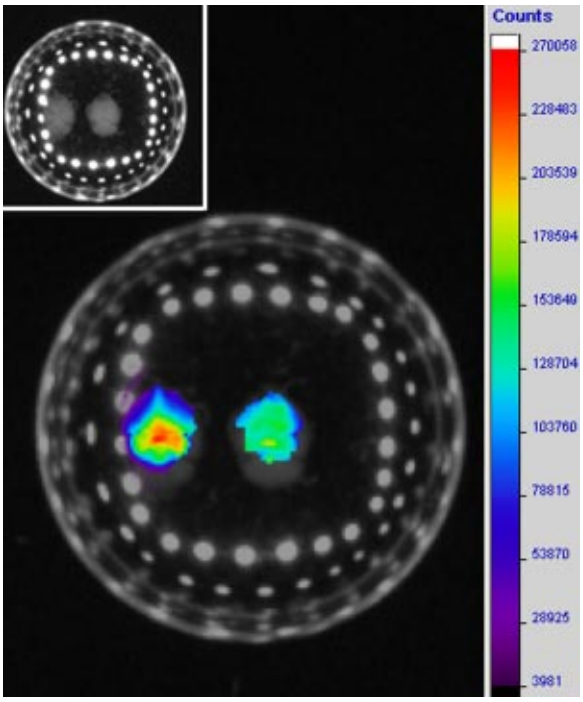

Fig. 3 Detection of Aβ in excised brains using the model compound Alexa Fluor 750-labeled BAM-10 antibody using the eXplore Optix. Postmortem brains from mice were fixed in 4% paraformaldehyde and incubated in Alexa Fluor 750-labeled antiamyloid antibody BAM-10. The left brain is from a PDAPP transgenic mouse, right is an age-matched nontransgenic control. The brains were glued to the bottom of a Petri dish, and submerged in PBS. Images were acquired using the eXplore Optix (Advanced Research Technologies, Inc.), using a picosecond-pulsed 750-nm laser. Integrated photon counts were pseudo-colored (scale bar on right) and overlaid upon a white light image (inset) of the sample. The plaque-containing brain on the left revealed a much higher fluorescent intensity at these wavelengths than the nontransgenic brain.

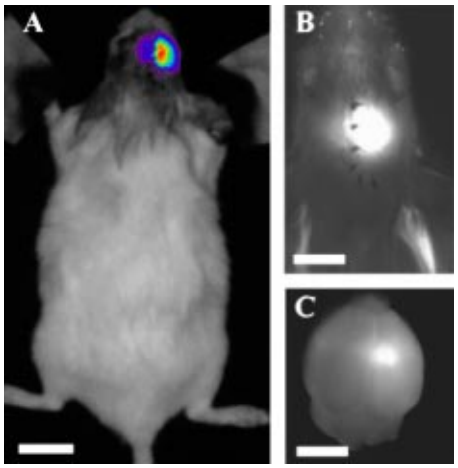

Fig. 4 Noninvasive detection of NIR fluorescence *in vivo* in the brain of an intact mouse. A bolus intracerebral injection of Alexa Fluor 750-labeled BAM-10 antibody (8 μL) was made in an anesthetized mouse in the right hemisphere several millimeters deep from the cortical surface. The skin was restored and sutured closed along the midline. Shortly thereafter, the anesthetized mouse was imaged using (a) the eXplore Optix and (b) the LI-COR Odyssey. Imaging was performed through the skin and skull in the intact, live animal with the focal plane set at eye level in the eXplore Optix imager and at 4 mm from the scanner surface of the Odyssey plate reader. The fluorescent signal was readily detected with both instruments, and was confined to the injected hemisphere. The mouse was sacrificed 24 h after injection, and the postmortem brain was extracted and fixed in 4% paraformaldehyde. (c) The isolated brain was imaged using the LI-COR Odyssey using a 3-mm focus offset from the scanner surface. The eXplore Optix image captured (a) at 0.5-mm resolution, (b) *in vivo* LI-COR image at 42-μm resolution, and (c) *ex vivo* brain image at 21 μm. Scale bars (a) 1.8 cm, (b) 1 cm, and (c) 5.5 mm.

brains of mouse models of Alzheimer's disease. The eXplore Optix instrument is capable of imaging an anesthetized but living animal, providing a platform ideal for *in vivo* drug studies and longitudinal studies using NIR readouts.

To evaluate the ability of these NIR fluorescence detection schemes to image fluorescence deep within the brain of a living animal noninvasively, we injected the NIR fluorophore Alexa Fluor 750 directly into the brain of a living 2.5-month-old transgenic (TgCRND-8) mouse.[20] The dye (conjugated to BAM-10 antibody) was injected into the brain using a Hamilton syringe through a small burr hole. The needle penetrated several millimeters into the brain, for deep injection of the fluorescent compound. The skin was closed with sutures over the midline of the mouse. The anesthetized mouse was then imaged using both the LI-COR and eXplore Optix detection platforms. Figure 4 shows the resultant scans. Both detection systems were able to image the fluorescence from within the brain with similar results. After 24 h the animal was sacrificed, and the brain was removed. Figure 4(c) shows a scan of the isolated brain using the LI-COR Odyssey, and demonstrates that the fluorescent bolus of Alexa Fluor 750 is still present within the brain, and easily detectable.

Despite our ability to detect fluorescence from deep within the brain after injecting directly labeled antibodies, we were unable to detect differences between APP overexpressing transgenic animals and aged-matched controls (data not shown). This result was not unanticipated as these labeling agents produce high background levels that are difficult to avoid, and the antibodies employed can lead to clearance of Aβ within the time required for nonspecific label washout.[21,22] Nonetheless, these results demonstrate that noninvasive detection of deep fluorescent signals can be obtained with two different instruments, showing promise for deep tissue imaging of plaques with an appropriate Aβ-targeting fluorophore based on intensity alone, with the expectation that tomographic reconstruction of the scattered signal will only improve the sensitivity.

4 Discussion

In this paper, we adapted our current imaging tools and employed existing commercial instruments to aid in the development and characterization of novel amyloid-imaging reagents for noninvasive optical detection of Alzheimer's pathology. We demonstrated that we can detect amyloid binding with specific NIR probes at either very high spatial resolution for histochemical confirmation, or lower resolution for noninvasive whole brain imaging. Fluorescent dye that was injected deep within the brain of a live animal could be readily detected noninvasively through the scalp and skull with two

Downloaded From: http://biomedicaloptics.spiedigitallibrary.org/ on 01/25/2016 Terms of Use: http://spiedigitallibrary.org/ss/TermsOfUse.aspx

Table 1 NIR imaging systems overview. Comparison of features and limitations of laser scanning microscopy (LSM) and commercial platforms (LI-COR Odyssey™ plate reader, ART eXplore Optix™, and the Perkin-Elmer ScanArray Express™).

	Light Source	Resolution (per pixel)/Scanable Area	Applications	Limitations
LSM	Pulsed, tunable diode laser (710 to 920 nm)	<1 μm/<0.25 cm^2	Tissue sections	Small sampling area
LI-COR Odyssey	cw laser diodes at 680 and 780 nm	>21 μm/441 cm^2	Tissue sections, *ex vivo* samples, live intact animals	Lacks fluorescence lifetime and tomography capabilities
eXplore Optix	Pulsed diode laser at 750 nm	>0.5 mm/168 cm^2	*Ex vivo* samples, live intact animals, fluorescence lifetime imaging	3-mm detector offset excludes collection of nonscattered light—excludes imaging histological sections
ScanArray Express	cw lasers at 488, 543, and 633 nm	>5 μm/18 cm^2	Tissue sections, conventional fluorophores	Physical design for only 1×3 slides

different commercial imaging systems. An overview and assessment of the NIR capabilities of the devices reported here is presented in Table 1.

The potential impact of noninvasive optical imaging of AD pathology is large. While recent progress in the development of PET ligands for amyloid imaging in humans is encouraging,[8,9,19] there are several disadvantages to this approach. PET imaging requires radioactivity, is expensive, and is available only at specialized centers. An optical technique would overcome each of these obstacles and would enable more widespread and accessible detection platforms for both early diagnosis of the disease, and evaluation of anti-Aβ therapeutics in clinical trials. While optical brain imaging is subject to many of the same obstacles of achieving high resolutions through the skin and skull as conventional noninvasive techniques, the qualitative answers that a detectable fluorescent probe could provide in the near future bears great significance toward detection and treatment of diseases that are currently regarded as pathologically undiagnosable in living people.

While the advantages of NIR wavelengths for deep tissue imaging have been long appreciated, the applications have mostly been limited to detection of intrinsic absorption of hemoglobin.[23–25] Capitalizing on NIR fluorescence detection will have advantages over absorption measurements since the use of optical filters to separate the excitation light from the emission light will increase the SNR of the measurements. For this reason, a great deal of interest has been expressed recently in using fluorescent contrast agents with excitation and emission wavelengths in the NIR region.[26–29] With inevitable enhancements in detector sensitivity and diffuse optical tomographic reconstruction algorithms, NIR imaging of fluorescent probes bears the potential for eventually producing 3-D quantitative images.[14,30]

The next critical element for successful noninvasive imaging of Alzheimer-related pathology is the development of specific amyloid-binding ligands that get into the brain and have the appropriate spectral properties. Recent progress has been made in developing radioligands for PET imaging that enter the CNS and target amyloid deposits specifically.[9,19] These agents are fluorescent, and have enabled multiphoton imaging of senile plaques in mouse models of AD. Two of the most promising agents, MeO-XO4 and PIB, were derived from the fluorescent parent compounds congo red and thioflavin T, respectively.[9,19] These compounds are fluorescent in the blue region; we expect that attempts to red-shift the fluorescent properties of these dyes to the NIR spectrum will be successful. Alternatively, existing NIR chromophores can be derivatized to enable amyloid binding and passage across the BBB. A superior putative NIR labeling agent would be able to cross the BBB, label Aβ deposits without inducing clearance, and have a significant shift in quantum efficiency or emission spectrum between the bound and unbound dyes. Clever chemical synthetic strategies are necessary for this goal, but should be feasible.

In summary, there are a variety of techniques available for both characterizing NIR fluorophores invasively or in tissue sections, as well as for noninvasive detection of signals in intact animals. This paper presented our progress toward noninvasive detection of Aβ plaques in transgenic mouse models of AD using model compounds. Successful development of amyloid-targeting reagents can now be evaluated easily in the laboratory and applied to the mouse models. Ultimately, it should be possible to detect AD pathology noninvasively in humans using optical techniques.

References

1. W. R. Markesbery, ''Neuropathological criteria for the diagnosis of Alzheimer's disease,'' *Neurobiol. Aging* **18**, S13–19 (1997).
2. B. T. Hyman, ''The neuropathological diagnosis of Alzheimer's disease: clinical-pathological studies,'' *Neurobiol. Aging* **18**, 527–532 (1997).
3. B. T. Hyman and J. Q. Trojanowski, ''Consensus recommendations for the postmortem diagnosis of Alzheimer disease from the National Institute on Aging and the Reagan Institute Working Group on diagnostic criteria for the neuropathological assessment of Alzheimer disease,'' *J. Neuropathol. Exp. Neurol.* **56**, 1095–1097 (1997).
4. D. J. Selkoe, ''Physiological production of the beta-amyloid protein and the mechanism of Alzheimer's disease,'' *Trends Neurosci.* **16**, 403–409 (1993).
5. S. E. Arnold, B. T. Hyman, J. Flory, A. R. Damasio, and G. W. Van Hoesen, ''The topographical and neuroanatomical distribution of neu-

Downloaded From: http://biomedicaloptics.spiedigitallibrary.org/ on 01/25/2016 Terms of Use: http://spiedigitallibrary.org/ss/TermsOfUse.aspx

rofibrillary tangles and neuritic plaques in the cerebral cortex of patients with Alzheimer's disease,'' *Cereb. Cortex* **1**, 103–116 (1991).
6. G. Kelenyi, ''Thioflavin S fluorescent and Congo red anisotropic stainings in the histologic demonstration of amyloid,'' *Acta Neuropathol. (Berl)* **7**, 336–348 (1967).
7. J. Q. Trojanowski, M. L. Schmidt, R. W. Shin, G. T. Bramblett, D. Rao, and V. M. Lee, ''Altered tau and neurofilament proteins in neuro-degenerative diseases: diagnostic implications for Alzheimer's disease and Lewy body dementias,'' *Brain Pathol.* **3**, 45–54 (1993).
8. K. Shoghi-Jadid, G. W. Small, E. D. Agdeppa, V. Kepe, L. M. Ercoli, P. Siddarth, S. Read, N. Satyamurthy, A. Petric, S. C. Huang, and J. R. Barrio, ''Localization of neurofibrillary tangles and beta-amyloid plaques in the brains of living patients with Alzheimer disease,'' *Am. J. Geriatr. Psychiatry* **10**, 24–35 (2002).
9. W. E. Klunk, H. Engler, A. Nordberg, Y. Wang, G. Blomqvist, D. P. Holt, M. Bergstrom, I. Savitcheva, G. F. Huang, S. Estrada, B. Avsen, M. L. Debnath, J. Barletta, J. C. Price, J. Sandell, B. J. Lopresti, A. Wall, P. Kovivisto, G. Antoni, C. A. Mathis, and B. Langstrom, ''Imaging brain amyloid in Alzheimer's disease using the novel PET tracer, PIB,'' *Ann. Neurol.* **55**, 781–789 (2004).
10. C. A. Mathis, B. J. Bacskai, S. T. Kajdasz, M. E. McLellan, M. P. Frosch, B. T. Hyman, D. P. Holt, Y. Wang, G. F. Huang, M. L. Debnath, and W. E. Klunk, ''A lipophilic thioflavin-T derivative for positron emission tomography (PET) imaging of amyloid in brain,'' *Bioorg. Med. Chem. Lett.* **12**, 295–298 (2002).
11. B. J. Bacskai, G. A. Hickey, J. Skoch, S. T. Kajdasz, Y. Wang, G. F. Huang, C. A. Mathis, W. E. Klunk, and B. T. Hyman, ''Four-dimensional multiphoton imaging of brain entry, amyloid binding, and clearance of an amyloid-beta ligand in transgenic mice,'' *Proc. Natl. Acad. Sci. U.S.A.* **100**, 12462–12467 (2003).
12. B. J. Bacskai, W. E. Klunk, C. A. Mathis, and B. T. Hyman, ''Imaging amyloid-beta deposits in vivo,'' *J. Cereb. Blood Flow Metab.* **22**, 1035–1041 (2002).
13. V. Ntziachristos, C. Bremer, and R. Weissleder, ''Fluorescence imaging with near-infrared light: new technological advances that enable in vivo molecular imaging,'' *Eur. Radiol.* **13**, 195–208 (2003).
14. J. P. Culver, A. M. Siegel, J. J. Stott, and D. A. Boas, ''Volumetric diffuse optical tomography of brain activity,'' *Opt. Lett.* **28**, 2061–2063 (2003).
15. R. B. Schulz, J. Ripoll, and V. Ntziachristos, ''Noncontact optical tomography of turbid media,'' *Opt. Lett.* **28**, 1701–1703 (2003).
16. K. Hsiao, P. Chapman, S. Nilsen, C. Eckman, Y. Harigaya, S. Younkin, F. Yang, and G. Cole, ''Correlative memory deficits, Abeta elevation, and amyloid plaques in transgenic mice,'' *Science* **274**, 99–102 (1996).
17. D. Games, D. Adams, R. Alessandrini, R. Barbour, P. Berthelette, C. Blackwell, T. Carr, J. Clemens, T. Donaldson, F. Gillespie, T. Guido, S. Hagoplan, K. Johnson-Wood, K. Kahn, M. Lee, P. Leibowitz, I. Lieberburg, S. Little, E. Masliah, L. McConlogue, M. Montoya-Zavala, L. Mucke, L. Paganini, E. Penniman, M. Power, D. Schenk, P. Seubert, B. Snyder, F. Soriano, H. Tan, J. Vitale, S. Wadsworth, B. Wolozin, and J. Zhao, ''Alzheimer-type neuropathology in transgenic mice overexpressing V717F beta-amyloid precursor protein,'' *Nature (London)* **373**, 523–527 (1995).
18. W. E. Klunk, Y. Wang, G. F. Huang, M. L. Debnath, D. P. Holt, and C. A. Mathis, ''Uncharged thioflavin-T derivatives bind to amyloid-beta protein with high affinity and readily enter the brain,'' *Life Sci.* **69**, 1471–1484 (2001).
19. W. E. Klunk, B. J. Bacskai, C. A. Mathis, S. T. Kajdasz, M. E. McLellan, M. P. Frosch, M. L. Debnath, D. P. Holt, Y. Wang, and B. T. Hyman, ''Imaging Abeta plaques in living transgenic mice with multiphoton microscopy and methoxy-X04, a systemically administered Congo red derivative,'' *J. Neuropathol. Exp. Neurol.* **61**, 797–805 (2002).
20. M. A. Chishti, D. S. Yang, C. Janus, A. L. Phinney, P. Horne, J. Pearson, R. Strome, N. Zuker, J. Loukides, J. French, S. Turner, G. Lozza, M. Grilli, S. Kunicki, C. Morissette, J. Paquette, F. Gervais, C. Bergeron, P. E. Fraser, G. A. Carlson, P. S. George-Hyslop, and D. Westaway, ''Early-onset amyloid deposition and cognitive deficits in transgenic mice expressing a double mutant form of amyloid precursor protein 695,'' *J. Biol. Chem.* **276**, 21562–21570 (2001).
21. B. J. Bacskai, S. T. Kajdasz, M. E. McLellan, D. Games, P. Seubert, D. Schenk, and B. T. Hyman, ''Non-Fc-mediated mechanisms are involved in clearance of amyloid-beta in vivo by immunotherapy,'' *J. Neurosci.* **22**, 7873–7878 (2002).
22. B. J. Bacskai, S. T. Kajdasz, R. H. Christie, C. Carter, D. Games, P. Seubert, D. Schenk, and B. T. Hyman, ''Imaging of amyloid-beta deposits in brains of living mice permits direct observation of clearance of plaques with immunotherapy,'' *Nat. Med.* **7**, 369–372 (2001).
23. M. Tamura, Y. Hoshi, and F. Okada, ''Localized near-infrared spectroscopy and functional optical imaging of brain activity,'' *Philos. Trans. R. Soc. London, Ser. B* **352**, 737–742 (1997).
24. J. P. Culver, T. Durduran, C. Cheung, D. Furuya, J. H. Greenberg, and A. G. Yodh, ''Diffuse optical measurement of hemoglobin and cerebral blood flow in rat brain during hypercapnia, hypoxia and cardiac arrest,'' *Adv. Exp. Med. Biol.* **510**, 293–297 (2003).
25. B. Chance, S. Nioka, S. Sadi, and C. Li, ''Oxygenation and blood concentration changes in human subject prefrontal activation by anagram solutions,'' *Adv. Exp. Med. Biol.* **510**, 397–401 (2003).
26. V. Ntziachristos, C. H. Tung, C. Bremer, and R. Weissleder, ''Fluorescence molecular tomography resolves protease activity in vivo,'' *Nat. Med.* **8**, 757–760 (2002).
27. M. A. O'Leary, D. A. Boas, X. D. Li, B. Chance, and A. G. Yodh, ''Fluorescence lifetime imaging in turbid media,'' *Opt. Lett.* **21**, 158–160 (1996).
28. E. M. Sevick-Muraca, J. S. Reynolds, T. L. Troy, G. Lopez, and D. Y. Paithankar, ''Fluorescence lifetime spectroscopic imaging with measurements of photon migration,'' *Ann. N.Y. Acad. Sci.* **838**, 46–57 (1998).
29. E. M. Sevick-Muraca, J. P. Houston, and M. Gurfinkel, ''Fluorescence-enhanced, near infrared diagnostic imaging with contrast agents,'' *Curr. Opin. Chem. Biol.* **6**, 642–650 (2002).
30. A. H. Hielscher, A. Y. Bluestone, G. S. Abdoulaev, A. D. Klose, J. Lasker, M. Stewart, U. Netz, and J. Beuthan, ''Near-infrared diffuse optical tomography,'' *Dis. Markers* **18**, 313–337 (2002).

Downloaded From: http://biomedicaloptics.spiedigitallibrary.org/ on 01/25/2016 Terms of Use: http://spiedigitallibrary.org/ss/TermsOfUse.aspx